JOURNAL OF SOLID STATE CHEMISTRY 93, 202–211 (1991)

X-Ray Study of the Average Structures of Cu_2Se and $Cu_{1.8}S$ in the Room Temperature and the High Temperature Phases

K. YAMAMOTO AND S. KASHIDA

Department of Physics, Niigata University, Ikarashi, Niigata, 950-21, Japan

Received August 27, 1990; in revised form January 22, 1991

The structures of the antifluorite-type copper chalcogenides Cu_2Se and $Cu_{1.8}S$ were studied using single crystal X-ray diffraction data both below and above the transition point. Using the cubic indexing main reflections, the average structures of the compounds were refined by least squares methods: a face-centered arrangement of the chalcogen atoms was assumed and copper atoms were distributed at the tetrahedral, trigonal, and octahedral interstitial sites, and their relative populations were refined. The tetrahedral and trigonal sites are populated by copper atoms at both room temperature and high temperature phases. The octahedral site is not populated in the room temperature phase of either Cu_2Se and $Cu_{1.8}S$. Contrary to the recent EXAFS analysis, however, this site is populated in the high temperature phase of Cu_2Se. From the population data, the drift pathway of copper ions was discussed.

1. Introduction

Copper chalcogenides are well known as fast ion conductors; the compounds exhibit wide deviation from stoichiometry as expressed by the formula $Cu_{2-x}S$ or $Cu_{2-x}Se$. Their high temperature structure is characterized by immobile anion "cages" which have cubic or hexagonal close-packed layers; copper atoms are randomly distributed at tetrahedral, trigonal, and octahedral interstices of the anions.

Upon cooling, the compounds undergo phase transitions below which the cations are ordered in the long range scale. This ordering of the cation subsystem is followed by the distortion of the anion cages. A number of studies have been accumulated about the variety of the ordered structures (*1*). Suffering from the complexity of the twinnings, however, the low temperature structures are not satisfactorily understood.

In the present study, we concentrated upon the chalcogenide compounds $Cu_{1.8}S$ (digenite) and Cu_2Se (berzelianite), which have a cubic antifluorite type base structure: the stoichiometric compound Cu_2S (chalcocite) has a different structure which is based on a hexagonal lattice (*1*). At room temperature, digenite crystals exhibit satellite reflections indicating uniaxial modulation of the lattices along the body diagonal of the cube (*2–4*). The periodic distortion is attributed to the ordering of vacant cation sites; its wavelength is commensurate or incommensurate with the basic lattice, depending upon the composition (*5*). The room temperature structure of cuprous selenide, Cu_2Se is also characterized by a periodic distortion due to vacancy arrays at the tetrahedral cation sites (*6–8*).

In order to obtain detailed information about the structure, we have collected single crystal diffraction data both below and

0022-4596/91 $3.00

above the transition points. By comparing the structures of both phases of the same sample, it would be possible to minimize systematic errors in the data set. Precise information about the average structure of the room temperature phase is of fundamental importance for the analysis of the modulated structure. In the refinement, the Fourier synthesis was used effectively as well as the normal least squares method. For the high temperature phase a least squares program was used which incorporates the treatment of anharmonic thermal vibrations.

2. Experimental

The samples were prepared by direct reaction of sulfur or selenium with copper. The weighted elements, sulfur (99.999%) or selenium (99.999%) and copper (99.99%) were sealed in an evacuated silica tube. The mixture of the sulfur compound was heated to 700°C and the selenium compound was heated to 900°C, for about 1 week and then cooled to room temperature over about 4 hr. The obtained crystals were shiny black and had distorted cubooctahedrons terminated by $(111)_c$ and $(100)_c$ planes.

Preliminary checks of the samples were made by the precession photographs. The stoichiometric selenide crystals showed unique superlattice reflections suggesting a lattice octuple along the ⟨111⟩ direction. However, crystals of the sulfides with nominal component $Cu_{1.8}S$ showed, in the ⟨110⟩ photographs, several kinds of satellite reflections which correspond to lattices multiplied by 4 or 5 ~ 6 along ⟨111⟩. Anilite has a quadruple superlattice structure, crystals with 5 ~ 6a period are classified as digenite. Other crystals had a different pattern corresponding to djurleite structure (*1*). As a representative of the sulfide compounds, we have taken digenite, which has a 5a structure. Preliminary checks of the samples by the DTA method showed that the transition point of $Cu_{1.8}S$ is about 80°C and that of Cu_2Se is about 130°C.

Untwinned crystals which had a nearly spherical shape were selected for the intensity measurement. Crystals were not ground further, because both the sulfide and the selenide copper compounds are very sensitive to mechanical strains. The dimensions of the samples used were given in Table I.

The measurement of the intensity was done using an automatic single crystal diffractometer assembled in our laboratory. As an X-ray source a Mo tube was used at 40 kV × 20 mA; the incident X-ray beam was monochromated by a flat graphite crystal. The main part of the diffractometer consisted of a Huber four-circle goniometer. The distance between the crystal and the detector slit was 275 mm and the receiving slit used was 8 mm × 8 mm. The samples were mounted on a goniometer head and set in a controlled air stream. The temperature of the samples was kept constant within 2 K by a PID controller.

The unit cell parameters were derived by a least-squares method from 18 reflections within the range of $23° < 2\theta < 38°$. The obtained unit cell parameters are given in Table I. The integrated intensity was collected by the omega scan method. Since the observed Bragg reflections usually had smeared long tails, the scan range was taken wider than the usual measurement as 4°, and the scanning rate was 1°/min. Background counts were measured for 20 sec at each limit of the scan range.

The intensities of reflections in a hemisphere of the reciprocal space within a 2θ value of 60° were collected. Three standard reflections were monitored every 100 reflections. There was no significant change in the intensity of the standard reflections in the measurement at room temperature phase. There was also no significant change in the measurement of Cu_2Se at 160°C. In the case of $Cu_{1.8}S$ at 120°C, however, during a period of 48 hr, the intensity of the standard reflections decreased about 10 ~30%. This may be attributed to the oxidation of the sulfur atoms or the metastability of the high temperature structure to decompose.

TABLE I

CRYSTAL DATA FOR Cu_2Se AND $Cu_{1.8}S$ (LOW), AT 300 K, Cu_2Se (HIGH) AT 433 K, AND $Cu_{1.8}S$ (HIGH) AT 93 K

Sample dimensions	
Cu_2Se $0.18 \times 0.25 \times 0.28$ mm^3	$Cu_{1.8}S$ $0.13 \times 0.15 \times 0.16$ mm^3
Absorption coefficients	
Cu_2Se $\mu = 421$ cm^{-1} and $\mu R \sim 6$	$Cu_{1.8}S$ $\mu = 244$ cm^{-1} and $\mu R \sim 1.8$
Agreement between equivalent F_o^2	(No. of independent reflections)
Cu_2Se_{low} 13.8% (26)	$Cu_{1.8}S_{low}$ 7.1% (23)
Cu_2Se_{high} 9.7% (26)	$Cu_{1.8}S_{high}$ 10.4% (23)
Lattice constants	
Cu_2Se_{low} 5.694(7) (average value)	$Cu_{1.8}S_{low}$ 5.564(17)
Cu_2Se_{high} 5.787(2)	$Cu_{1.8}S_{high}$ 5.582(9)

In total, 539 (Cu_2Se) and 530 ($Cu_{1.8}S$) reflections were scanned, of which the intensity is less than the standard deviation were discarded. The data were corrected for the Lorentz and polarization effects. Absorption correction was made by assuming spherical shapes of the specimens, and equivalent reflections were averaged. No corrections were made for the decay of the intensity in $Cu_{1.8}S$ at 120°C, since the correction is not easy (the decay depends upon the reflection index and increases with the 2θ value). We have scanned sequentially the reflections in a full hemisphere, whereas the needed data are only 1/48 and obtained by averaging; therefore, the decay is considered not to cause any serious error. The numbers of independent reflection thus obtained were given in Table I. The values of the absorption coefficients and the internal agreement factor of the observed equivalent reflections, which is defined by the equation $\Sigma||F_o| - |\bar{F}_o||/\Sigma|F_o|$, are also given in Table I.

3. Analysis of Experimental Results and Discussion

3.1 Room Temperature Phase

The average structures of both Cu_2Se and $Cu_{1.8}S$ were determined by taking into account only the intensity of the fundamental reflections, that of the satellite reflections was ignored. The analysis was done assuming the space group $Fm3m$, a face-centered lattice of the anions and refining occupation parameters of the anions. The least squares program "RADIEL" (*9*) was used. In the refinement, all reflections were given unit weight, the scattering factors used are those listed in International Tables for X-Ray Crystallography (1974) (*10*).

Three models were examined: in the first model only the tetrahedral 8(*c*) sites are populated by copper atoms; in the second model two sites are populated (the tetrahedral site and the trigonal 32(*f*) site); in the third model the octahedral 4(*b*) site is allocated besides the tetragonal and trigonal sites.

The obtained *R*-factors and the relevant parameters are given in Table II,[1] where *R*

[1] A list of structure factors for all data sets have been deposited with the National Auxiliary Publication Service. See NAPS document No. 04865 for 13 pages of supplementary material from ASIS/NAPS, Microfiche Publications, P.O. Box 3515, Grand Central Station, New York, NY 10163. Remit in advance $4.00 for microfiche copy or for photocopy, $7.75 up to 20 pages plus $.30 for each additional page. All orders must be prepaid. Institutions and Organizations may order by purchase order. However, there is a billing and handling charge for this service of $15. Foreign orders add $4.50 for postage and handling, for the first 20 pages, and $1.00 for additional 10 pages of material, $1.50 for postage of any microfiche orders.

TABLE II

SUMMARY OF THE REFINEMENTS OF THE ROOM TEMPERATURE AVERAGE STRUCTURE OF Cu_2Se AND $Cu_{1.8}S$ AT 300 K

	Cu_2Se_{low}	
No. of parameters	R	R_w
6	0.065	0.039
Position	Population p	Thermal parameter U_{11}
Se at 0, 0, 0	1	0.39(2)
Cu at 1/4,1/4,1/4	0.37(7)	0.068(14)
and x,x,x x = 0.334(5)	0.63(11)	0.085(12)
	$Cu_{1.8}S_{low}$	
No. of parameters	R	R_w
6	0.068	0.073
Position	Population p	Thermal parameter U_{11}
S at 0, 0, 0	1	0.009(2)
Cu at 1/4,1/4,1/4	0.52(9)	0.069(5)
and x,x,x x = 0.326(2)	0.38(11)	0.031(2)

Note. Form of the harmonic temperature factor is $T_{harm} = \exp\{-2\pi^2 (h\,a^*)^2 U_{11} + \ldots\}$, where U_{11} etc. has the unit of $Å^2$.

$= \Sigma(|F_o| - |F_c|)/\Sigma|F_o|$ and R_w $[\Sigma\, w(|F_o| - |F_c|)^2/\Sigma\, w|F_o|^2]^{1/2}$ and $w = \{\sigma(F_o)^2\}^{-1}$.

For both compounds Cu_2Se and $Cu_{1.8}S$ the one-site (tetrahedral) model gave R-factors of about 20%; large deviations from this model were deduced from the difference Fourier map which showed large residual electron density at the trigonal sites. A significant improvement of the R-factors was obtained in the two-site model. The difference Fourier maps (Figs. 1b and 2b) showed no peak at the octahedral sites, and the third, three-site model, did not yield any improvement in the R-factors. Therefore, we have concluded that the octahedral site is not populated in the room temperature phase. The refined occupation ratios of the cations at the tetragonal and trigonal sites are 0.37 and 0.63 for Cu_2Se and 0.52 and 0.38 for $Cu_{1.8}S$, respectively.

Recently, Vucic *et al.* (*6*) proposed a model for the superstructure of Cu_2Se, where half of the copper atoms are in tetrahedral sites so as to form a zincblende structure; the remaining tetragonal sites are only two-thirds occupied and other copper atoms are in octahedral sites. The authors of (*8*) suggested another model where tetrahedral vacancies form a $\sqrt{3} \times \sqrt{3}$ lattice in the (111) layer at every four layers along the ⟨111⟩ direction.

The superstructure of the nonstoichiometric $Cu_{2-x}S$ is also attributed to an ordered array of vacancies at cation sites, but until now no detailed structure model was presented for digenite. Koto and Morimoto (*11*) studied the superstructure of anilite $Cu_{1.75}S$, which is also a modification of the antifluorite type: the structure belongs to the orthorhombic space group *Pnma* and the unit cell is composed of $\sqrt{2} \times \sqrt{2} \times 2$ cubic subcells containing 16 chemical units.

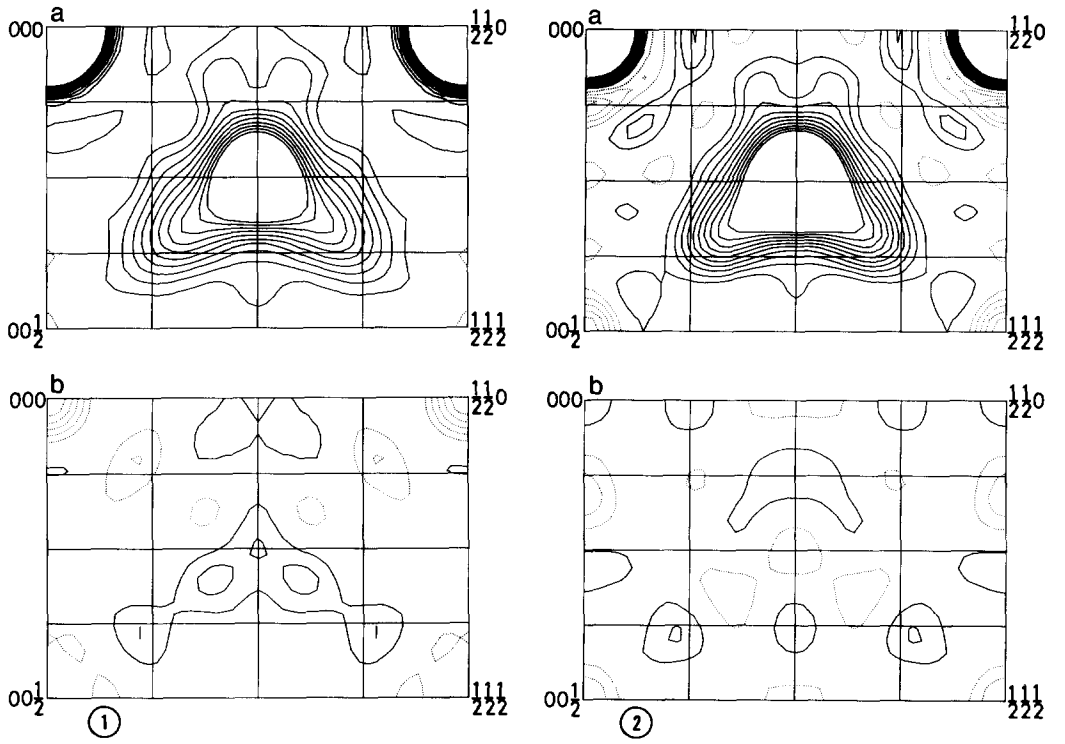

FIGS. 1 AND 2. (a) Fourier maps of the average structure in the (110) plane of Cu_2Se and $Cu_{1.8}S$ in the room temperature phase. (b) Difference Fourier maps calculated by the two-site model. Contours are drawn at intervals of 1 e $Å^{-3}$ (a) and 0.5 e $Å^{-3}$ (b); solid lines indicate electron excess, and dashed lines electron deficiency. For clarity the contour lines exceeding 10 e $Å^{-3}$ are not drawn.

The present results of the average occupation of the cation sites can be compared with those of anilite, where 8/32 = 0.25 copper atoms are in tetrahedral sites and 20/32 = 0.63 atoms are in triangular sites.

Realistic models for the low temperature superlattice structure of the copper chalcogenides, which reproduce the intensity of the satellite reflections, the average population numbers of the cations sites deduced here, and the Fourier maps given in Figs. 1a and 2a are desired. A further investigation is now in progress along this line.

3.2 High Temperature Fast-ion-Conducting Phase

Two different types of analysis were tried for this phase. In the first approach, as in the analysis of the room temperature phase, the split atom method was used along with hormonic temperature factors. In the second approach, anharmonic vibration of the atoms was taken into account. A least squares program "LINKT80" (*12*) was used, which incorporates Willis' formalism of the anharmonic temperature factors (*13*): the effective one-particle potential function which governs the motion of mobile ions is expanded up to the fourth order, as

$$V(u) = V_0 + 1/2\, B^{jk}u_j u_k + 1/3\, C^{jkl}u_j u_k u_l + 1/4\, Q^{jklm}u_j u_k u_l u_m, \quad (1)$$

where u represents deviation from the equilibrium position and B^{jk}, C^{jkl}, and Q^{jklm} are the second, third, and fourth order coefficients which are to be refined.

We added a small modification to the program so as to incorporate a refinement with the Gram–Charlier expansion (*14*): the probability density function was expanded up to the fourth order using the gaussian function $p_o(u)$

$$p(u) = p_o(u)\,[1 + 1/3!\,C^{jkl}H_{jkl}(u) + 1/4!\,Q^{jklm}H_{jklm}(u)], \quad (2)$$

where C^{jkl} and Q^{jklm} are the third and fourth order coefficients of the expansion which are to be refined, and H_{jkl} and H_{jklm} are the derivatives expressed by the Hermite polynomials. From the probability density function, the potential V can be calculated by the formula (*14*)

$$V(u) = -kT \ln \{p(u)/p(o)\}. \quad (3)$$

The refined R-factors and the relevant parameters such as the population numbers of the sites are given in Table III.[1]

In the analysis with the harmonic approximation, the one-site model did not fit the experimental results. The two-site model gave fairly low R-factors. In the anharmonic model, the Gram–Charlier expansion yielded lower R-factors and lesser residual electron density compared with those given by Willis' treatment. This fact may suggest that the approximation $V/kT \ll 1$ is not valid in the fast-ion-conducting phase. The detailed result of the Willis treatment is not given here.

(*a*) *Cu_2Se*. The harmonic two sites (tetrahedral and trigonal) model gives the same order of R-factor with the anharmonic model with the Gram–Charlier expansion for the atoms in the tetrahedral site. The difference Fourier maps obtained by these models show small residual electron density at the octahedral 4(*b*) sites and 24(*e*) sites (cf. Fig. 3c). The relative intensity of these two sites is higher at 4(*b*) sites, and an addition of 4(*b*) sites to the refinement yields a significant drop of R-factor from 0.060 to 0.032.

Heyding and Murray (*16*) studied the structure of a nonstoichiometric compound, $Cu_{1.8}Se$, which remains cubic to room temperature. They concluded that copper atoms are randomly distributed over the tetrahedral and trigonal sites with weight 5.2 and 2.0, respectively; the values can be compared with the present results.

(*b*) *$Cu_{1.8}S$*. The anharmonic model gives a lower R-factor compared with those of the harmonic two-site model. A further drop of the R-factor is obtained by applying the anharmonic treatment to the sulfur atom. In this case, the residual electron density is larger in the 24(*e*) site (cf. Fig. 4c). An addition of the 24(*e*) site in the refinement yields a slight drop of R-factors from 0.069 to 0.063, but an addition of the 4(*b*) site is not successful. As the amount of available reflection data is small, this drop is not significant according to the Hamilton test program (*15*). However, the final difference Fourier map is improved and contains no peak exceeding 1.5 e/Å (cf. Fig. 4b).

Morimoto and Kullerud (*3*) studied the high temperature structure of $Cu_{1.8}S$. They proposed a model where sulfur atoms form an fcc lattice and copper atoms are allocated at general positions 192(*c*), with $x = 0.31$, $y = 0.30$, and $z = 0.29$. We have examined their model; the obtained R-factor is about 0.17 and not better than that of the two site model.

3.3 Concluding Remarks

In the analysis of the high temperature phase, the harmonic multisite model and the anharmonic Gram–Charlier expansion give similar R-factors for similar numbers of the adjustable parameters. It may be worthwhile from our diffraction data to add some comments about the drift path of the mobile ions. Figure 5 shows the plot of the potential functions which were deduced using Eq. (3) and the electron density in the Fourier maps.

In Cu_2Se, as Figs. 3a and 3c show, the

TABLE III

SUMMARY OF THE REFINEMENTS OF THE HIGH TEMPERATURE STRUCTURE OF Cu_2Se AT 433 K AND $Cu_{1.8}S$ AT 393 K

Cu_2Se_{high}

Model 1 (harmonic)

No. of parameters	R	R_w
6	0.060	0.031
Position	Population p	Thermal parameter U_{11}
Se at 0, 0, 0	1	0.042(2)
Cu at 1/4,1/4,1/4	0.64(12)	0.069(11)
and x,x,x x = 0.322(9)	0.36(14)	0.066(19)

Model 2 (harmonic)

No. of parameters	R	R_w
8	0.032	0.020
Position	Population p	Thermal parameter U_{11}
Se at 0, 0, 0	1	0.045(1)
Cu at 1/4,1/4,1/4	0.47(10)	0.057(10)
and x,x,x x = 0.315(6)	0.48(11)	0.083(10)
and 1/2, 0, 0	0.05(1)	0.177(77)

Model 3 (anharmonic, Gram–Charlier)

No. of parameters	R	R_w			
10	0.037	0.032			
	Population	Thermal parameters			
Position	p	U_{11}	C_{123}	Q_{1111}	Q_{112}
Se at 0, 0, 0	1	0.043(19)	(harmonic)		
Cu at 1/4,1/4,1/4	0.95	0.137(24)	7.6(1.1)	0.18(14)	0.45(28)
and 1/2, 0, 0	0.05	0.207(118)	—	−3.0(3.6)	6.0(11.)

$Cu_{1.8}S_{high}$

Model 1 (harmonic)

No. of parameters	R	R_w
6	0.099	0.113
Position	Population p	Thermal parameter U_{11}
S at 0, 0, 0	1	0.008(3)
Cu at 1/4,1/4,1/4	0.68(14)	0.105(10)
and x,x,x x = 0.322(9)	0.22(14)	0.028(12)

TABLE III (*Continued*)

Model 2 (anharmonic, Gram–Charlier)					
No. of parameters	R	R_w			
8	0.069	0.069			
	Population	Thermal parameters			
Position	p	U_{11}	C_{123}	Q_{1111}	Q_{112}
S at 0, 0, 0	1	0.060(16)	—	0.47(25)	0.45(19)
Cu at 1/4,1/4,1/4	0.9	0.152(36)	8.5(2.1)	−0.50(15)	0.72(58)

Model 3 (anharmonic, Gram–Charlier)					
No. of parameters	R	R_w			
11	0.063	0.060			
	Population	Thermal parameters			
Position	p	U_{11}	C_{123}	Q_{1111}	Q_{112}
S at 0, 0, 0	1	0.055(19)			
Cu at 1/4,1/4,1/4	0.87(4)	0.150(28)	—	0.35(22)	0.35(16)
and x,0,0 x = 0.288(26)	0.03(2)	0.002(250)	7.2(2.1)	−0.58(15)	0.64(47)

Note. Form of the anharmonic temperature factor in Gram–Charlier expansion is $T_{\text{anharm}} = T_{\text{harm}} \times \{1 + (2\pi i)^3/3! \times C_{ijk}h_ih_jh_k + (2\pi i)^4/4! \times Q_{ijkl}h_ih_jh_kh_l\}$, where T_{harm} has the same form as in Table II.

electron density of copper ions has a long tail toward the octahedral site. The result is consistent with recent experimental and simulation studies (*18, 19*) of the fluorite structure which showed that the minimum energy drift path is through (0.5, 0.5, 0.5). Our result is, however, inconsistent with recent studies by EXAFS and neutron diffraction (*20, 21*), where it was concluded that the octahedral site is not populated.

For $Cu_{1.8}S$, the situation is similar to that of Cu_2Se, but a slightly different pathway may be expected. The difference Fourier map (Fig. 4c) displays a maximum around (0.5, 0.5, 0.29), a position fairly distant from the center of the sulfur octahedron. The density of copper atoms displayed in the Fourier map (Fig. 4a) has lobes along the $[001]_c$ axis as well as $[111]_c$. Our least squares refinement suggests an anharmonic motion of the immobile sulfur atom. Therefore, in $Cu_{1.8}S$, the pathway may be of more short and straight: the cations move from a tetrahedral site to another tetrahedral site more directly, pushing sulfur atoms outward. The pathway will depend on several factors such as the ratio of atomic radii and masses of mobile and immobile ions, or the deviation of the concentration of the mobile ions from stoichiometry. A recent simulation study by Kaneko and Ueda (*22*) showed that the pathway between the tetrahedral sites is direct when the repulsion between the cations and anions is soft, and that the pathway is pushed toward the octahedral site when the repulsion is strong. It may be interesting to notice that the extension of the electron cloud of the selenium atom is wider than that of the sulfur atom (cf. Figs. 3a and 4a). It is consistent with the result of the simulation

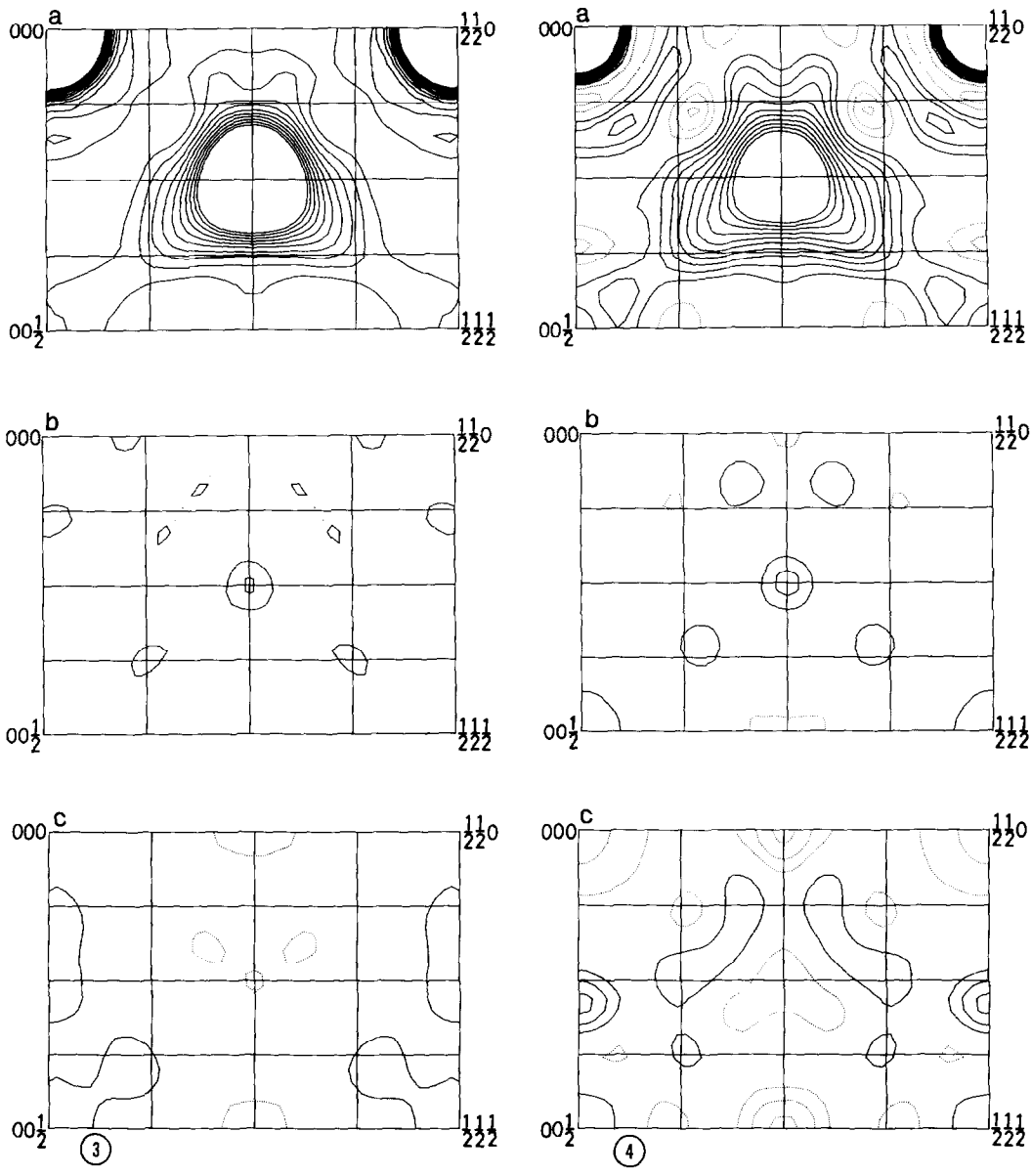

FIGS. 3 AND 4. Fourier maps (a), and final difference Fourier maps (b) in the (110) plane in the high temperature phase of Cu_2Se (Fig. 3) and $Cu_{1.8}S$ (Fig. 4) Difference Fourier maps (c) are obtained by the two-site model (tetrahedral and trigonal sites), see text. Contours are drawn at intervals of 1 e $Å^{-3}$ (a) and 0.5 e $Å^{-3}$ (b), (c); solid lines indicate electron excess, and dashed lines electron deficiency. For clarity the contour lines exceeding 10 e $Å^{-3}$ are not drawn.

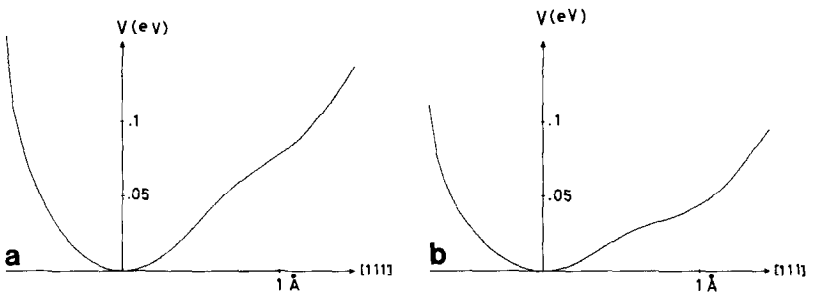

FIG. 5. Potential curves of the copper ions along the $[111]_c$ direction estimated from the densities in the Fourier maps. (a) Cu_2Se, (b) $Cu_{1.8}S$; the origin is at the tetrahedral site. The activation energy for copper diffusion is reported as about 0.24 eV for both Cu_2Se and Cu_2S (*18*).

study. However, further detailed studies are needed in order to clarify the pathways of the mobile ions.

Acknowledgments

The authors thank Professor K. Tanaka of Nagoya Institute of Technology for providing us his software program "LINKT80." They also thank Dr. Y. Watanabe of the Institute for Materials Research, Tohoku University for providing useful information about his software program for data acquisition.

References

1. H. T. EVANS, JR., *Am. Mineral.* **66,** 807 (1981).
2. G. DONNAY, J. D. H. DONNAY, AND G. KULLERUD, *Am. Mineral.* **43,** 228 (1958).
3. N. MORIMOTO AND G. KULLERUD, *Am. Mineral.* **48,** 110 (1963).
4. J. N. GRAY AND ROY CLARKE, *Phys. Rev. B* **33,** 2056 (1986).
5. N. MORIMOTO AND K. KOTO, *Am. Mineral.* **55,** 106 (1970).
6. Z. VUCIC, O. MILAT, V. HORVATIC, AND Z. OGORELEC, *Phys. Rev. B* **24,** 5398 (1981).
7. O. MILAT AND Z. VUCIC, *Solid State Ionics.* **23,** 37 (1987).
8. S. KASHIDA AND J. AKAI *J. Phys. C* **21,** 5329 (1988).
9. H. COPPENS AND W. C. HAMILTON, *Acta Crystallogr. Sect. A* **26,** 70 (1970).
10. "International Tables for X-Ray Crystallography," Vol. IV, The Kynoch Press, Birmingham (1974).
11. K. KOTO AND N. MORIMOTO, *Acta Crystallogr. Sect. B* **26,** 915 (1970).
12. K. TANAKA AND F. MARUMO, *Acta Crystallogr. Sect. A* **39,** 631 (1983).
13. B. T. M. WILLIS AND A. W. PRYOR, "Thermal Vibration in Crystallography," Cambridge Univ. Press, Cambridge (1975).
14. U. H. ZUCKER AND H. SCHULZ, *Acta Crystallogr. Sect. A* **38,** 563 (1982).
15. W. C. HAMILTON, *Acta Crystallogr.* **8,** 502 (1965).
16. R. D. HEYDING AND R. M. MURRAY, *Can. J. Chem.* **54,** 841 (1975).
17. K. OKAMOTO AND S. KAWAI, *Jpn. J. Appl. Phys.* **8,** 718 (1973).
18. K. KOTO, H. SCHULZ AND R. A. HUGGINS, *Solid State Ionics* **1,** 355 (1980).
19. M. KOBAYASHI, K. ISHIKAWA, F. TACHIBANA, AND H. OKAZAKI, *Phys. Rev. B* **38,** 3050 (1988).
20. J. B. BOYCE, T. M. HAYES AND J. C. MIKKELSEN, JR., *Solid State Ionics* **5,** 497 (1981).
21. M. H. DICKENS, M. T. HUTCHINGS, AND C. SMITH, *J. Phys. C.* **15,** 4043 (1982).
22. Y. KANEKO AND A. UEDA, *J. Phys. Soc. Jpn.*, **57,** 3064 (1988).